JCI insight

RESEARCH ARTICLE

Excess growth hormone suppresses DNA damage repair in epithelial cells

Vera Chesnokova,[1] Svetlana Zonis,[1] Robert Barrett,[2,3] Hiraku Kameda,[1] Kolja Wawrowsky,[1] Anat Ben-Shlomo,[1] Masaaki Yamamoto,[1] John Gleeson,[2,3] Catherine Bresee,[4] Vera Gorbunova,[5] and Shlomo Melmed[1]

[1]Pituitary Center, [2]Board of Governors Regenerative Medicine Institute, [3]F. Widjaja Foundation Inflammatory Bowel and Immunobiology Research Institute, Department of Medicine, and [4]Biostatistics and Bioinformatics Research Institute, Cedars-Sinai Medical Center, Los Angeles, California, USA. [5]Department of Biology, University of Rochester, Rochester, New York, USA.

Growth hormone (GH) decreases with age, and GH therapy has been advocated by some to sustain lean muscle mass and vigor in aging patients and advocated by athletes to enhance performance. Environmental insults and aging lead to DNA damage, which – if unrepaired – results in chromosomal instability and tumorigenesis. We show that GH suppresses epithelial DNA damage repair and blocks ataxia telangiectasia mutated (ATM) kinase autophosphorylation with decreased activity. Decreased phosphorylation of ATM target proteins p53, checkpoint kinase 2 (Chk2), and histone 2A variant led to decreased DNA repair by nonhomologous end-joining. In vivo, prolonged high GH levels resulted in a 60% increase in unrepaired colon epithelial DNA damage. GH suppression of ATM was mediated by induced tripartite motif containing protein 29 (TRIM29) and attenuated tat interacting protein 60 kDa (Tip60). By contrast, DNA repair was increased in human nontumorous colon cells (hNCC) where GH receptor (GHR) was stably suppressed and in colon tissue derived from *GHR*$^{-/-}$ mice. hNCC treated with etoposide and GH showed enhanced transformation, as evidenced by increased growth in soft agar. In mice bearing human colon GH-secreting xenografts, metastatic lesions were increased. The results elucidate a mechanism underlying GH-activated epithelial cell transformation and highlight an adverse risk for inappropriate adult GH treatment.

Introduction

Growth hormone (GH) secreted by the pituitary gland acts through insulin-like growth factor–1 (IGF-1) to regulate tissue growth and metabolism (1–4). GH also acts independently of IGF-1 in regulating bone, muscle, and liver tissue functions (5–8). In adults, GH is only approved as a physiologic replacement for pituitary-deficient individuals or to improve AIDS-associated muscle wasting (9). The age associated somatopause characterized by physiologic decline of circulating GH occurs due to diminished pituitary GH production (10, 11). GH replacement in adults with proven GH deficiency results in loss of abdominal fat, increased muscle mass and energy, increased bone mineral density, and improved exercise capacity (12–14). Based on these GH effects reported in pituitary-deficient adults, recombinant human GH and GH-related products have been aggressively promoted in an attempt to reverse age-associated frailty in pituitary-replete healthy adults (15) and are also widely used to improperly enhance athletic performance (16). However, inappropriate treatment of otherwise healthy adults with GH produces modest changes in body composition with significant side effects, including arthritis, edema, insulin resistance, and heart disease (12, 16, 17). Furthermore, evidence from animal and human studies support a direct role for GH in the progression of neoplastic epithelial growth (18–20). Excess pituitary tumor GH secretion in acromegaly results in soft tissue overgrowth and increased adenoma formation in the colon, skin, thyroid, and prostate (21), and it is associated with increased risk for colorectal carcinoma (22, 23). GH triggers epithelial-to-mesenchymal transition, creating a proneoplastic mucosal environment (24–27). By contrast, abrogated GH signaling is associated with decreased cancer development in humans and in mice (20, 28–30). For example, short-stature humans harboring an inactivating mutation in the GH receptor (GHR) do not develop cancer (28), and GHR knockdown in human melanoma cells attenuates tumor progression (31).

Conflict of interest: The authors have declared that no conflict of interest exists.

Submitted: October 24, 2018
Accepted: December 20, 2018
Published: February 7, 2019

Reference information:
JCI Insight. 2019;4(3):e125762.
https://doi.org/10.1172/jci.insight.125762.

In view of widespread GH abuse, it is important to further examine mechanisms for protumorigenic GH actions. We recently showed that GH is induced in nonpituitary human breast and colon cells in response to activation of the p53/p21 pathway (32), which plays an important role in DNA damage response (DDR). Since we also demonstrated that GH, in turn, suppresses colon p53/p21 (24), we sought to determine whether GH regulates DDR.

Oncogenic mutations may be associated with inefficient repair of damaged DNA, and surveillance mechanisms detect DNA damage and exert DNA repair to maintain genomic stability. The Ser/Thr protein kinase ataxia telangiectasia mutated (ATM) is a key component of signaling pathways activated by DNA damage (33). ATM is activated in response to DNA strand breaks by Ser^{1981} autophosphorylation (34). Activated ATM triggers DDR (33), phosphorylates checkpoint kinase 2 (Chk2) to arrest cell proliferation (35), and phosphorylates p53 at Ser^{15}, resulting in its activation and stabilization (36). In turn, activated p53 drives cell cycle arrest, as well as promotion of DNA repair and programmed cell death (37). γ-Histone 2A variant (γH2AX) formed by ATM-induced Ser^{139} phosphorylation in response to double- or single-strand DNA breaks (33, 38, 39) is required for DNA repair protein assembly, as well as for activation of cell cycle checkpoint proteins (37, 40).

We show here that GH decreases ATM kinase activity and suppresses ATM autophosphorylation, with subsequently decreased H2AX and p53 phosphorylation in both normal colon cells and in human 3-dimensional intestinal organoids. In in vitro and in vivo models, GH induced tripartite motif containing 29 (TRIM29) (41) and suppressed tat interacting protein 60 kDa (Tip60), leading to ATM destabilization (42). GH treatment led to increased unrepaired DNA both in vivo and in vitro, likely due to decreased nonhomologous end-joining (NHEJ), and enhanced anchorage-independent growth of normal colon cells. In athymic mice bearing GH-secreting human colon HCT116 xenografts, metastatic lesions were more prevalent, and the number of metastases correlates strongly with the levels of circulating GH. The results indicate that suppression of DNA repair by GH may guide colon cells toward transformation, and they highlight an adverse risk for inappropriate adult GH administration.

Results

GH suppresses etoposide-induced DDR. To examine whether increased GH affects DDR, we employed topoisomerase II inhibitor etoposide to produce single- and double-stranded DNA breaks (43). We treated human nontumorous colon cells (hNCC) with 500 ng/ml GH for 6 hours and then induced DNA damage with 5 μM etoposide. After 24 hours, total ATM expression was seen to be unchanged, but levels of pATM were lower in cells treated with GH and etoposide, compared with cells treated with etoposide alone. Decreased ATM phosphorylation, in turn, resulted in decreased phosphorylation of its target protein p53. ATM also regulates DNA repair via Rad50 phosphorylation (44), and we found that levels of pRad50 were markedly lower after GH treatment (Figure 1A and Supplemental Figure 1A; supplemental material available online with this article; https://doi.org/10.1172/jci.insight.125762DS1). Together, these results suggest that GH suppresses DDR by decreasing ATM phosphorylation. Similar results were observed in nontumorous human mammary cells (MCF12A) and in colon adenocarcinoma HCT116 cells (Supplemental Figure 2, A and B).

At a later time point, 96 hours after etoposide treatment, we found comparable decreased pATM levels in GH-treated hNCC cells (Supplemental Figure 1D).

We also tested effects of etoposide in hNCC at earlier time points. In cells pretreated with GH for 6 hours and then treated with etoposide for 1 or 3 hours, we observed decreased ATM and p53 phosphorylation compared with cells treated solely with etoposide (Figure 1B and Supplemental Figure 1B). Chk2 phosphorylation was unchanged in response to GH 24 hours after etoposide treatment, but GH reduced Chk2 phosphorylation 3 hours after etoposide (Figure 1B and Supplemental Figure 1B), reflecting an earlier reduction in ATM phosphorylation.

Phosphorylation of H2AX is an early event in the double-strand break (DSB) response. Activated ATM phosphorylates H2AX, and γH2AX marks damaged DNA sites to activate DDR and promote DNA repair (45). We found decreased γH2AX in GH-treated hNCC cells 1, 3, 24, and 96 hours after etoposide (Figure 1, A and B, and Supplemental Figure 1, A, B, and D), with similar findings in GH-treated MCF12A and HCT116 cells 24 hours after etoposide (Supplemental Figure 2, A and B). Cotreating hNCC cells with etoposide and GH resulted in decreased aggregate measurements of γH2AX observed on immunocytochemistry slides, such as the number of γH2AX foci per nucleus and their intensity (Figure 1C and Supplemental Figure 3, A and B).

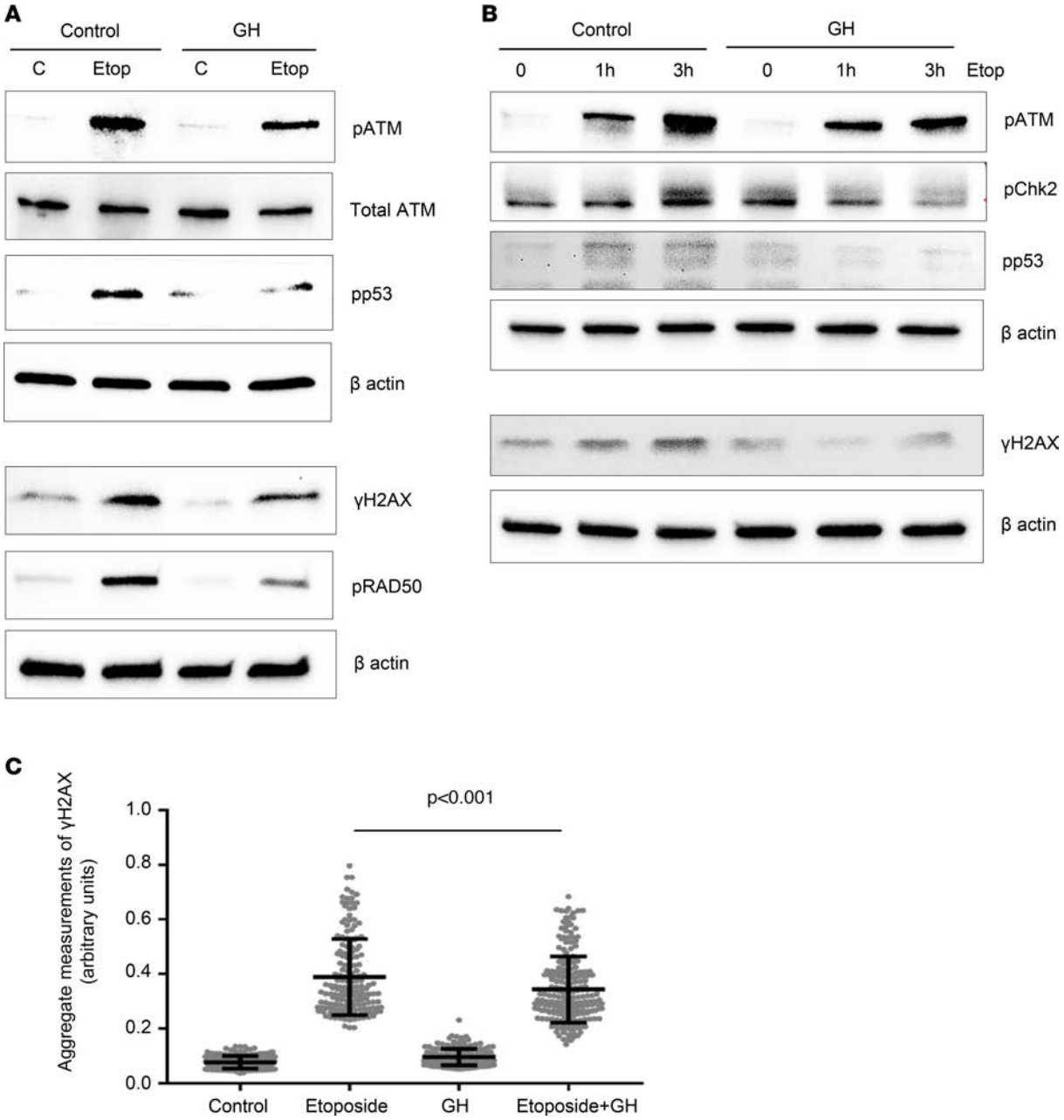

Figure 1. GH suppresses etoposide-induced DNA damage response (DDR) and increases unrepaired DNA damage. In all experiments, hNCC were pre-treated with 500 ng/ml GH for 6 h and then treated with 5 μM etoposide (Etop). (**A**) Western blot of hNCC harvested 24 hours after etoposide treatment. (**B**) Western blot of hNCC harvested 1 and 3 hours after etoposide treatment. Shown are representative results from 3–5 independent experiments. For **A** and **B**, quantification of protein expression is depicted in Supplemental Figure 1, A and B. (**C**) Aggregate measurements of γH2AX foci in hNCC harvested 24 hours after etoposide treatment. One dot represents measurements in a single nucleus; 20–30 nuclei per image and 5 images per group were analyzed. Differences were assessed by nonparametric Wilcoxon rank sum test.

Decreased γH2Ax in GH-treated cells may result from rapid repair of DNA damage or from DDR not fully activated in response to etoposide. We interpreted our results as indicating that GH decreases ATM phosphorylation (activation), which in turn leads to decreased phosphorylation of H2AX, p53, and Chk2 target proteins. In support of this interpretation, we observed that endogenous ATM kinase activity measured in hNCC exposed to GH was reduced by approximately 40% in response to etoposide (Figure 2, A and B, and Supplemental Figure 1C), indicating that DDR was not fully activated, thus allowing for decreased DNA damage repair and accumulated DNA damage. Indeed, employing the comet assay to assess DNA damage in nontumorous colon hNCC and mammary MCF12A cells, we observed that cells treated with both etoposide

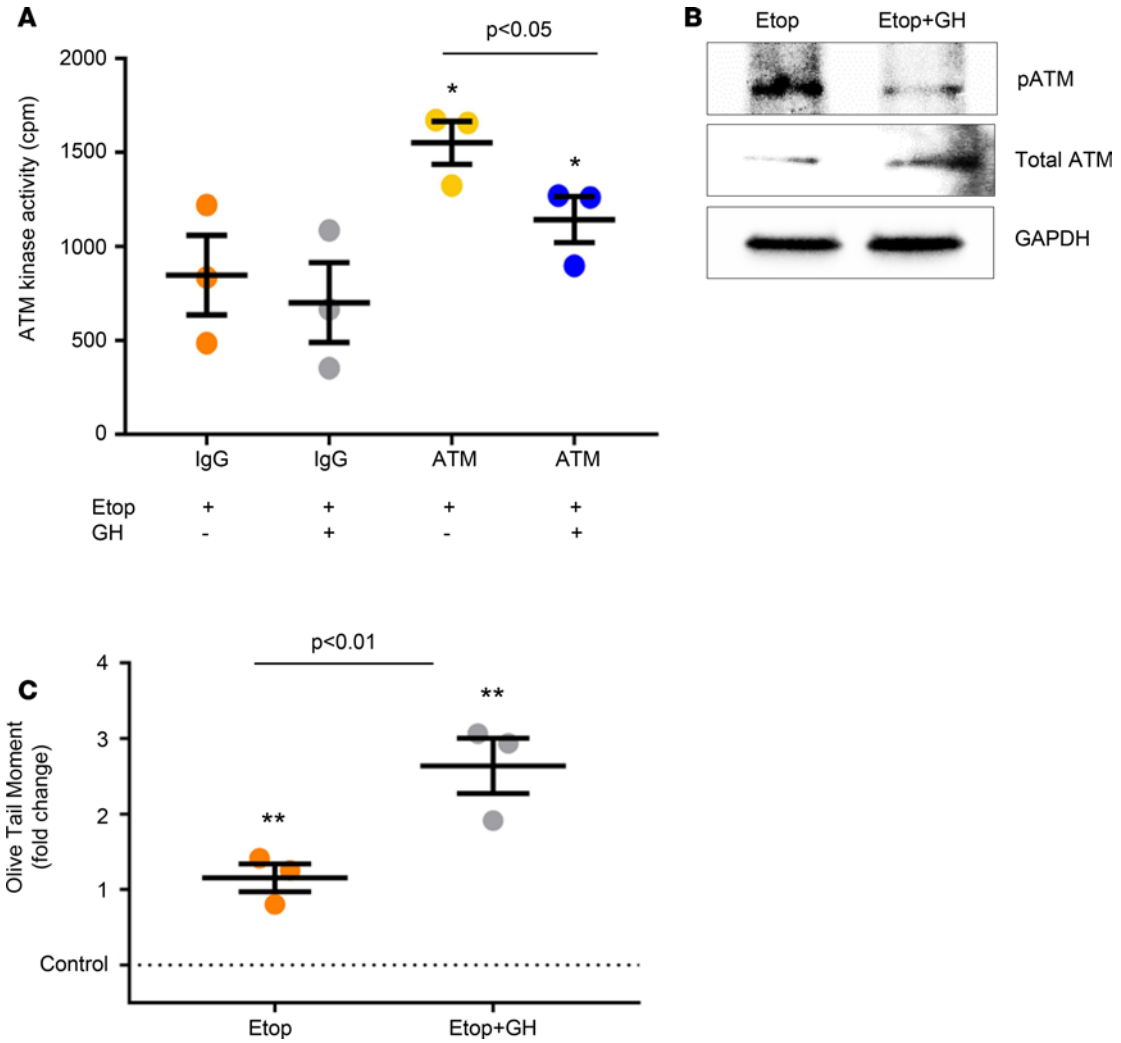

Figure 2. GH suppresses ATM kinase activity. (**A**) ATM kinase assay. hNCC were pretreated with GH and treated with etoposide for 3 hours. Cell extracts were immunoprecipitated with total ATM antibody. (**B**) Controls using IgG or in which the peptide was omitted were included. Assays were conducted in triplicate. Results shown are mean ± SEM of 3 independent experiments. Each dot represents 1 independent experiment. Data are graphed as fold-change, but statistical testing was performed on raw numbers. Differences were assessed with Tukey-adjusted mixed model regression. *$P < 0.0\,5$ vs. IgG + Etop. (**B**) For ATM kinase assay, Western blotting was used to detect total ATM or autophosphorylated ATM (phospho-Ser 1981) and to verify equal protein amount in the immunoprecipitated samples for each experiment. Representative blots are shown. Quantification of protein expression is depicted in Supplemental Figure 1C. (**C**) Comet assay of hNCC harvested 24 hours after etoposide treatment. Single-cell gel electrophoresis was conducted and Olive Tail Moments assessed on at least 200 cells/per slide for each experiment. Results shown are mean ± SEM. Control, untreated cells. **$P < 0.01$ vs. control. Differences were assessed with Tukey-adjusted mixed model regression.

and GH exhibit more unrepaired DNA damage vs. cells treated solely with etoposide (Figure 2C and Supplemental Figure 2C). By contrast, in cancerous HCT116 cells, the extent of DNA damage did not differ significantly between cells challenged with etoposide in the presence or absence of GH (Supplemental Figure 2C).

To elucidate mechanisms for DDR suppression by GH, we tested expression of proteins involved in ATM regulation. TRIM29 suppresses histone acetyltransferase Tip60 (46), which in turn acetylates ATM, inducing activation and autophosphorylation (42). Treatment of hNCC with etoposide or GH for 24 hours markedly enhanced TRIM29 expression, but addition of GH did not further increase high TRIM29 in etoposide-treated cells. By contrast, GH treatment decreased Tip60 expression in both control and etoposide-treated cells (Figure 3A and Supplemental Figure 4A). Comparable results were observed in HCT116 cells (Supplemental Figure 5), in which GH pretreatment increased TRIM29 expression and suppressed Tip60 in both control and etoposide-treated cells.

At earlier time points, at 1 and 3 hours after treatment, TRIM29 was markedly induced in cells treated with etoposide or GH only, but etoposide did not further induce TRIM29 in cells pretreated with GH (Fig-

ure 3B and Supplemental Figure 4B). Activated TRIM29 downregulated Tip60 in GH-treated cells (Figure 3B and Supplemental Figure 4B), which likely resulted in the observed decrease in ATM, H2AX, p53, and Chk2 phosphorylation in response to etoposide (Figure 1B). Thus, GH-induced TRIM29 and the resultant decreased Tip60 likely lead to decreased DDR activity.

A product of the multidrug resistance 1 (MDR1) gene protects cells from genotoxic effects of chemotherapy (47). We found that MDR1 was not changed in cells treated with GH or in cells overexpressing GH after etoposide treatment (Supplemental Figure 6), indicating that protective GH effects on DNA damaged cells are likely not mediated by GH-induced MDR1.

GH suppresses DDR in human intestinal organoids. We next examined effects of GH on DDR in human intestinal organoids by pretreating with GH overnight and then treating with etoposide for an additional 24 hours. While TRIM29 was induced by both etoposide and GH, Tip60 was suppressed by the addition of GH to etoposide (Figure 3C and Supplemental Figure 7A). Phosphorylation of ATM, H2AX, and p53 were markedly reduced in organoids treated with both GH and etoposide compared with organoids treated with etoposide only (Figure 3D and Supplemental Figure 7B).

We then tested the extent of DNA damage in organoids treated with 3 μM and 5 μM etoposide in the presence or absence of GH. Similar to its effects in hNCC, GH exacerbated DNA damage caused by both doses of etoposide treatment (Figure 3E). Levels of phosphorylated ATM, Rad50, p53, and H2AX were also accordingly decreased in organoids treated with GH (Supplemental Figure 8, A and B).

GH suppresses endogenous DDR and increases unrepaired DNA damage. After finding that GH suppressed etoposide-induced ATM kinase phosphorylation and prevented complete DDR activation, we tested whether GH also acts to alter baseline DDR. In hNCC treated with 500 ng/ml GH for 24 hours, GH induced TRIM29 expression while suppressing Tip60. Downregulation of Tip60, in turn, likely resulted in suppressed ATM phosphorylation, as we observed subsequent decreased phosphorylated H2AX, p53, and Rad50 in cells treated with GH (Figure 4A and Supplemental Figure 9A). Comet assay showed an increase of approximately 50% in baseline DNA damage (Figure 4B), indicating that GH also suppresses endogenous DDR and may lead to increased unrepaired DNA damage.

To test whether GH suppresses ATM kinase phosphorylation at lower doses, we treated hNCC cells with 100 ng/ml GH and harvested cells 24 hours later. ATM phosphorylation was also markedly suppressed even at this modest GH dose (Supplemental Figure 9C).

GH suppresses DDR via TRIM29/Tip60. As high TRIM29 may reduce ATM kinase activity by suppressing Tip60 (42), we generated hNCC stably expressing shTRIM29. In scrambled shRNA transfectants, GH induced TRIM29 and suppressed Tip60, and it also reduced phosphorylation of ATM. When TRIM29 was downregulated, Tip60 was significantly induced, likely as a result of TRIM29 suppression and independent of GH treatment. Induction of Tip60, in turn, was associated with increased pATM as compared with cells stably expressing scrambled RNA and treated with GH (Figure 4C and Supplemental Figure 9B). These results suggest that GH action on Tip60 and pATM requires TRIM29, at least under baseline conditions.

High GH action on TRIM29/Tip60 and DNA damage in vivo. We next considered whether high GH levels would similarly impact the TRIM29/Tip60 pathway in vivo. Athymic nude mice were injected with HCT116 cells stably infected with lentivirus-expressing murine GH (lentiGH) or empty vector (lentiV). lentiGH xenografts recapitulate the systemic GH increase, as observed in acromegaly, and lead to increased circulating GH (Supplemental Figure 10A). We found induced colon TRIM29 and suppressed Tip60 in 6 of 7 lentiGH mice (Figure 5A and Supplemental Figure 10C). As exogenous DNA damage was not triggered, levels of pATM were difficult to detect; however, we still observed decreased phosphorylation of p53 and Rad50, likely resulting from downregulation of endogenous pATM (Figure 5A and Supplemental Figure 10C). In randomly selected animals carrying the xenograft, hepatic TRIM29 was similarly upregulated and Tip60 downregulated (Figure 5B and Supplemental Figure 10D).

Thus, high levels of circulating GH results in downregulation of DDR. To assess the consequence of GH-induced DDR suppression, we examine DNA damage in the colon tissue of experimental mice. Detected by comet assay, animals with high-circulating GH demonstrate 61% ± 14.5% higher levels of unrepaired DNA damage as compared with controls (Figure 5C).

GH affects DDR through the GHR. To confirm that GH signaling activates TRIM29 and subsequently suppresses DDR, we pretreated hNCC with 20 mg/ml pegvisomant, a GHR antagonist (48), for 1 hour and then treated cells with 500 ng/ml GH and harvested them 24 hours later. In control cells, as expected, GH treatment induced TRIM29 with subsequent downregulated Tip60 and decreased phosphorylation of

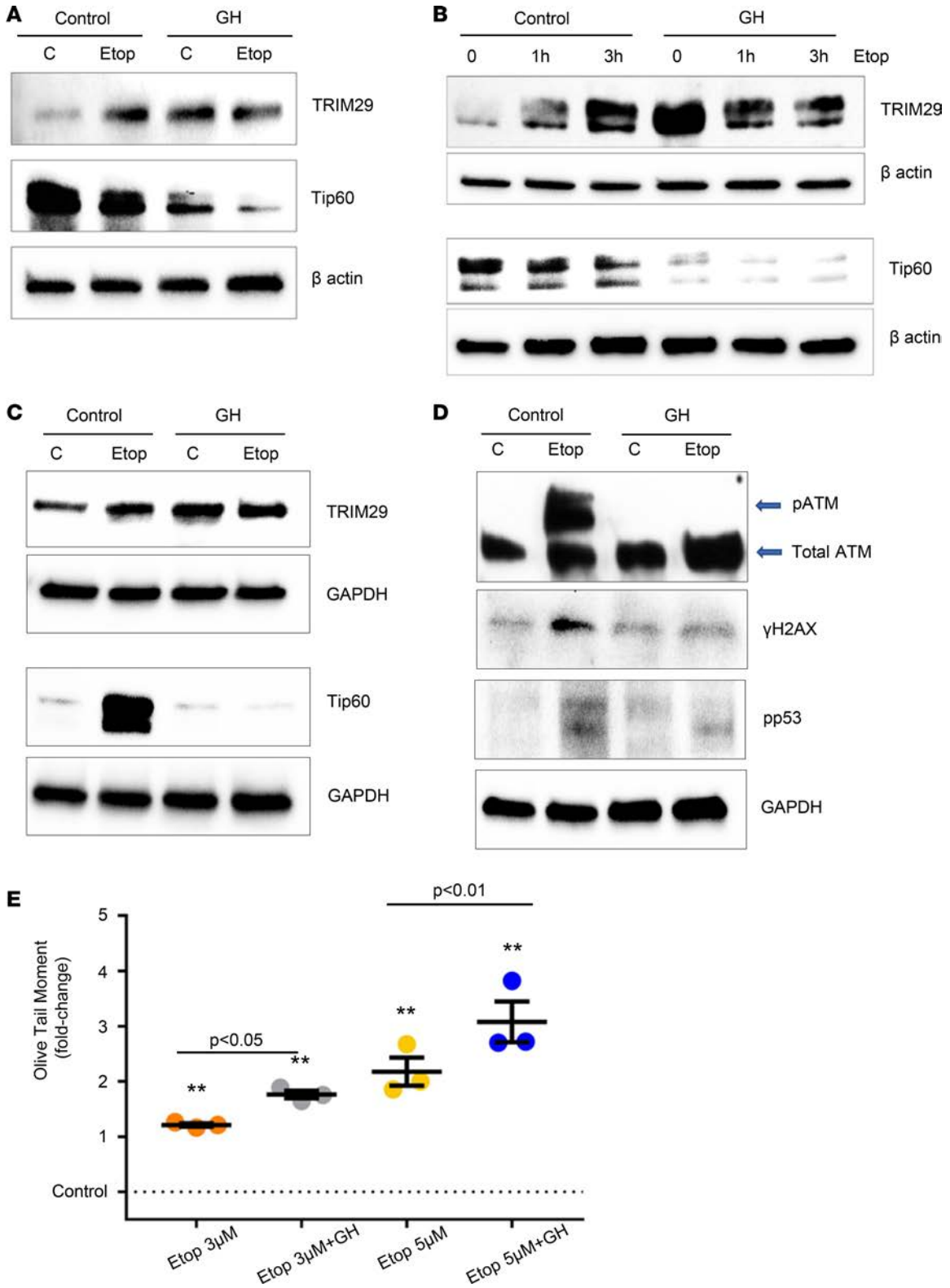

Figure 3. GH suppresses DDR in hNCC by inducing TRIM29 and suppressing Tip60. (**A** and **B**) hNCC were pretreated with 500 ng/ml GH and treated with 5 μM etoposide. Western blots of TRIM29 and Tip60 in hNCC harvested 24 hours (**A**) or 1 and 3 hours (**B**) after etoposide treatment. Shown are representative blots from at least 3 independent experiments. Quantification of protein expression is depicted in Supplemental Figure 4. (**C** and **D**) Three-dimensional intestinal organoids were pretreated with 500 ng/ml GH overnight, treated with etoposide for 24 hours, and harvested. Western blots of (**C**) TRIM29 and Tip60 and (**D**) DDR. Shown are representative blots from 3 independent experiments. Quantification of protein expression is depicted in Supplemental Figure 7. (**E**) Comet assay of organoids pretreated with 500 ng/ml GH, treated with 3 or 5 μM etoposide for 24 hours, and harvested. Results shown are mean ± SEM of 3 independent experiments. Differences were assessed with Tukey-adjusted mixed model regression. Control, untreated organoids. $^{**}P <$ 0.01 vs. control.

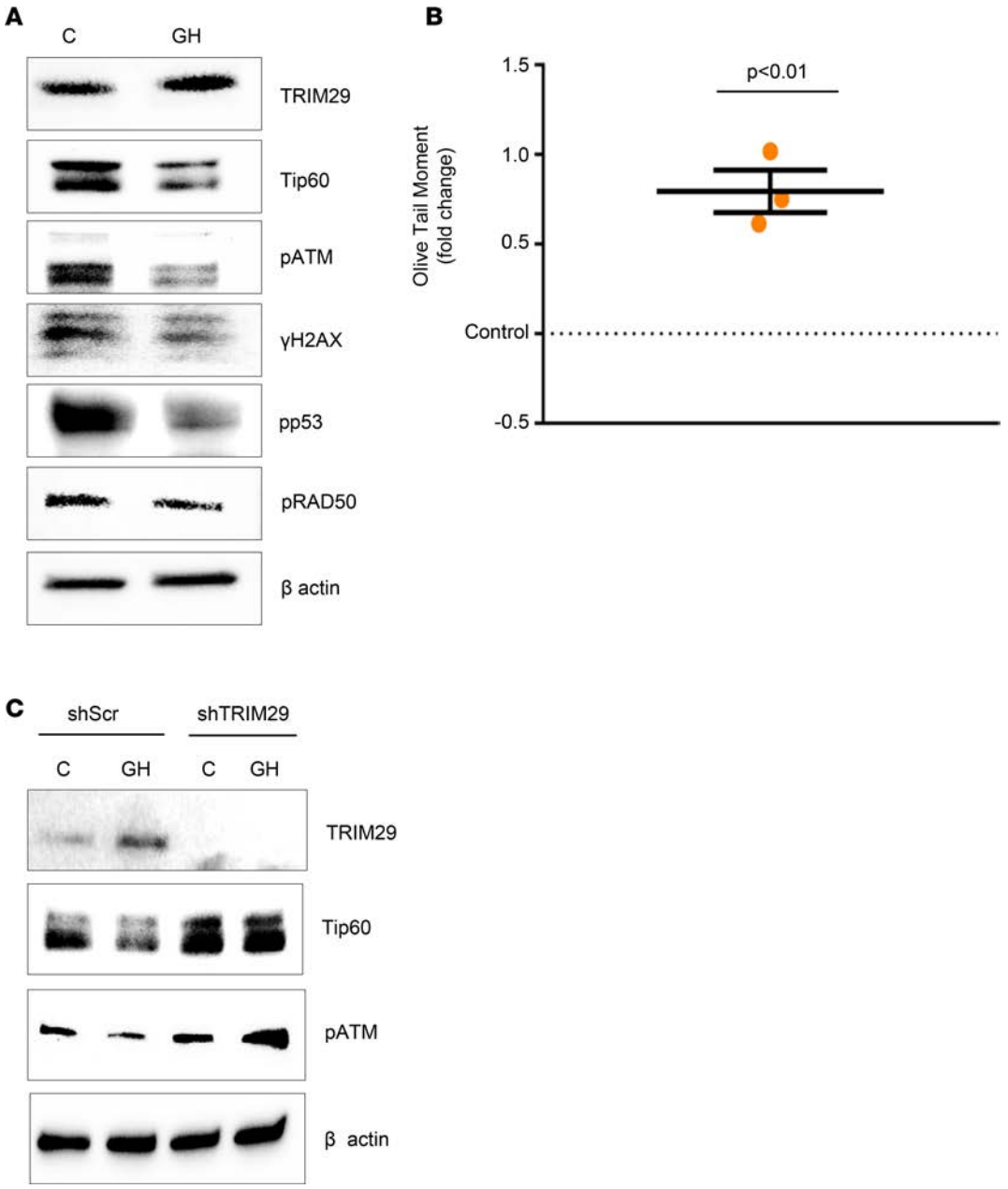

Figure 4. GH suppresses endogenous DDR via TRIM29/Tip60 pathway in vitro. (**A**) Western blot analysis of DDR and (**B**) comet assay in hNCC treated with 500 ng/ml GH for 24 hours. Results shown are mean ± SEM of 3 independent experiments. Controls represent untreated cells. Differences were assessed with Tukey-adjusted mixed model regression. (**C**) Western blot of hNCC stably expressing short hairpin scramble (shScr) or shTRIM29 RNAi and treated with 500 ng/ml GH for 24 hours. Shown are representative blots of at least 3 independent experiments. For **A** and **C**, quantification of protein expression is depicted in Supplemental Figure 9.

ATM and p53. By contrast, in cells treated with pegvisomant, blocking GH action led to downregulated TRIM29 and induction of Tip60, likely leading to the observed increased phosphorylated ATM and p53 (Figure 5A, Figure 6A, and Supplemental Figure 11A). These results indicate that GH, acting through the GHR, activates TRIM29 and suppresses DDR, leading to increased unrepaired DNA damage.

In support of this observation, we generated hNCC stably expressing shGHR and found a 30% decrease in DNA damage as assessed by comet assay compared with controls (Figure 6B). Similarly, abrogated GH signaling in *GHR*$^{-/-}$ mice resulted in decreased levels of unrepaired male colon DNA. In female *GHR*$^{-/-}$ mice, the difference did not reach significance (Figure 6C). In hNCC where GHR was suppressed, etoposide treatment resulted in marked pATM upregulation (Figure 6D and Supplemental Figure 11, B and C).

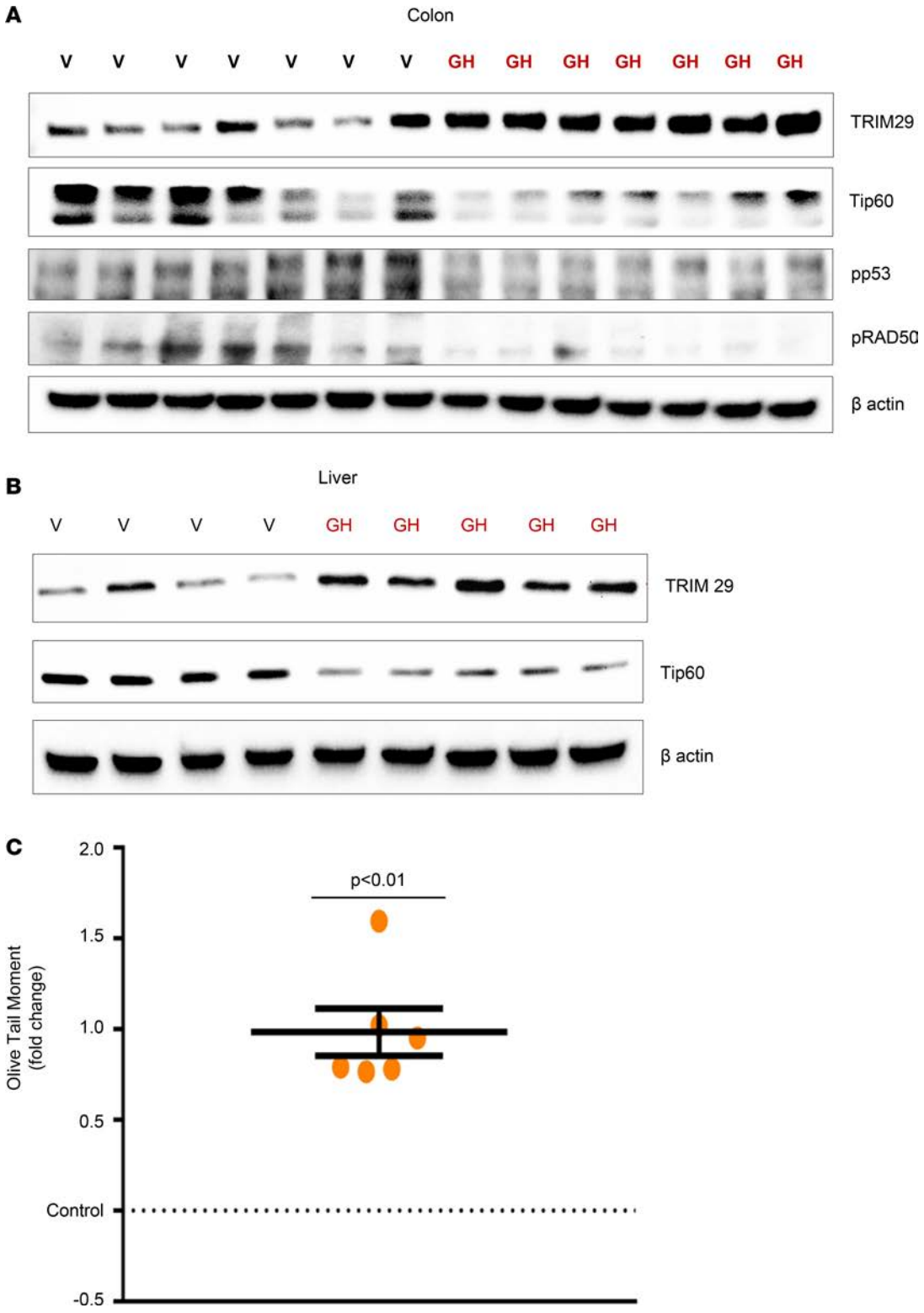

Figure 5. GH suppresses endogenous DDR via the TRIM29/Tip60 pathway in vivo. (**A–B**) Athymic nude mice were injected s.c. with 500,000 HCT116 cells stably infected with lenti mGH (GH) or lenti vector (lentiV) and sacrificed 5 weeks after injection. Western blot analysis of individual colon tissues (**A**) and liver tissues (**B**) derived from mice bearing xenograft tumors. Quantification of protein expression is depicted in Supplemental Figure10, C and D. (**C**) Comet assay in colon tissue of mice bearing HCT116 lenti mGH xenograft tumors. Results shown are mean ± SEM. *n* = 6 mice/group. Controls represent mice bearing lentiV xenografts.

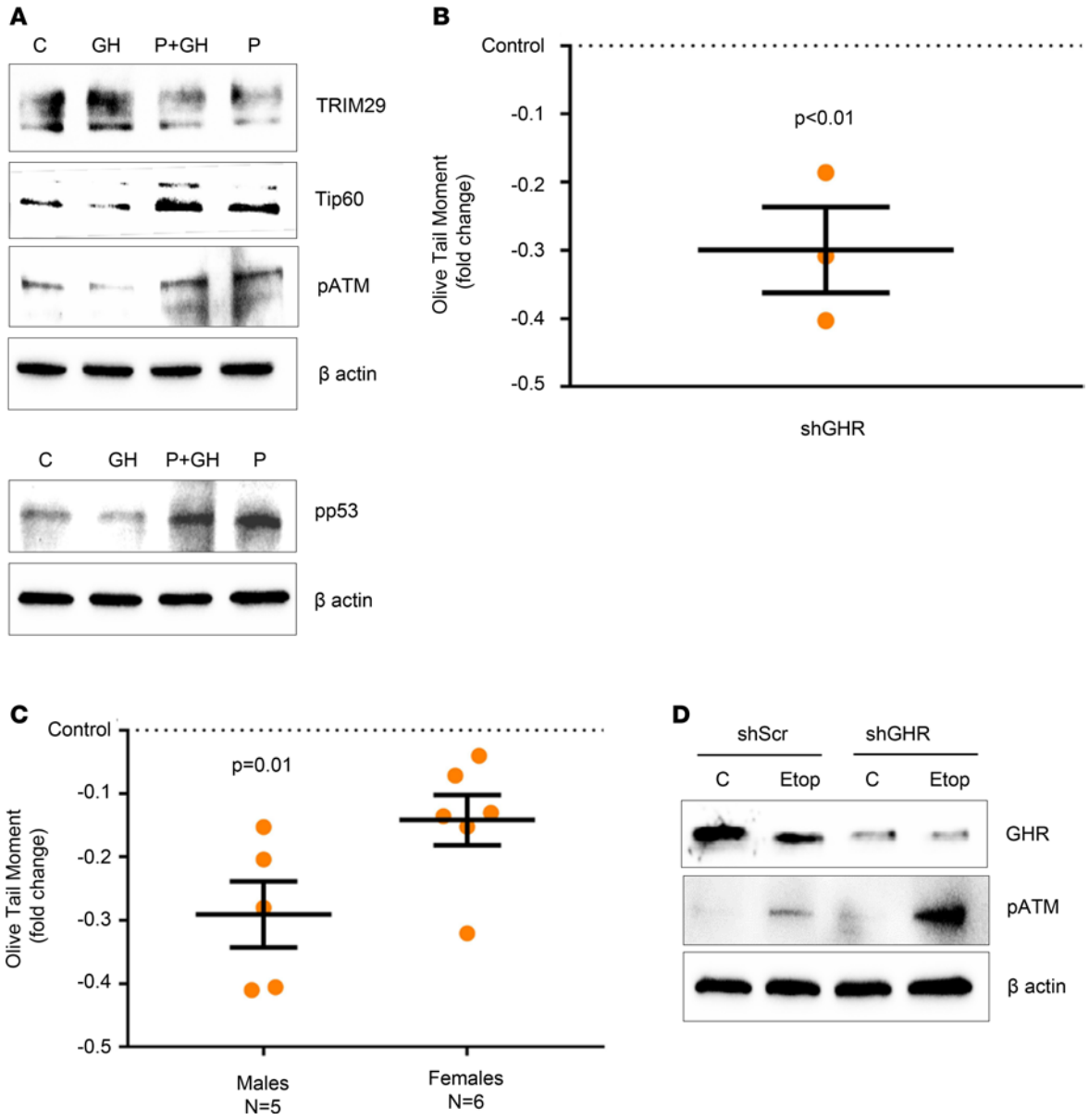

Figure 6. GH suppresses DDR via GHR. (**A**) Western blot of hNCC treated with 20 mg/ml pegvisomant (P) for 1 hour and then with 500 ng/ml GH for 24 hours; C, untreated control. This experiment was repeated 3 times with similar results; representative blots are shown. (**B**) Comet assay of hNCC stably expressing shGHR or scramble shRNAi (control). Results shown are mean ± SEM of 3 independent experiments. (**C**) Endogenous DNA damage in *GHR*$^{-/-}$ and WT colon tissue. WT(control) and *GHR*$^{-/-}$ mice were paired for analysis according to age and sex. Results shown are mean ± SEM (each dot represents 1 pair). For **B** and **C**, differences were assessed with Tukey-adjusted mixed model regression. (**D**) Western blot of hNCC stably expressing shGHR or scramble shRNAi and treated with 5 μM etoposide for 24 hours. Representative blots from 3 independent experiments are shown. For **A** and **D**, quantification of protein expression is depicted in Supplemental Figure 11, A and C.

GH attenuates DNA repair. As the DDR pathway is not fully activated in the presence of GH, we sought to examine whether GH affects NHEJ or homologous recombination (HR). Rapid DSB repair is mediated principally via NHEJ (49); HR occur with DNA damage at DNA replication forks (33, 50, 51). We measured rejoining of DSB repair reporters integrated into genomic DNA of hNCC (52) by cotransfecting these stable transfectants with plasmid encoding I-SceI endonuclease to induce DSBs, as well as with plasmid encoding DsRed to control for transfection efficiency; then we treated these transfectants with 500 ng/ml GH and assessed the results after 4 days. NHEJ efficiency was 35% ± 3.3% lower in cells treated with GH ($P < 0.05$) (Figure 7, A and B). We also observed a small but consistent decrease in HR efficiency (11% ± 2.04%, $n = 6$ independent experiments) 5 days after GH treatment.

As the catalytic subunit of DNA-dependent protein kinase (DNA-PKcs) is required for NHEJ repair, we examined effects of GH on this protein. Similar to ATM, DNA-PKcs is phosphorylated in response to DNA damage (33, 53). We found that GH suppressed phosphorylation of this protein in hNCC (Figure 7C and Supplemental Figure 12), implying that lower NHEJ efficiency in the presence of GH may be attributed to decreased DNA-PKcs activation.

GH action on proliferation, cell cycle, survival, and anchorage-independent growth. We tested GH action on hNCC proliferation when pretreated with GH for 6 hours and then treated with 5 μM etoposide. Seventy-two hours after the beginning of etoposide treatment, no difference was observed in cells incorporating BrdU among cells treated with etoposide only vs. both GH and etoposide (35.6% ± 7.2% vs. 33% ± 5.5%, respectively).

We examined GH effects on cell cycle progression. hNCC and HCT116 were plated in full medium, and when cells reached approximately 60% confluency, medium was changed to serum free with 0.1% BSA, and 500 ng/ml of GH was added. After a 6-hour incubation, cells were treated with 5 μM etoposide for 24 hours. Cells were then harvested, fixed in 70% ethanol, stained with propidium iodine, and analyzed by FACS in triplicate. In hNCC, GH treatment resulted in a modest 8% ± 2.7% increase in the number of cells in S-phase compared with untreated cells. In cells treated with GH and etoposide, the number of cells in S-phase was 20.7% ± 4.3% higher than in cells treated with etoposide only. These results indicate that GH reduced replication delay caused etoposide-induced DNA damage. No significant cell cycle changes were observed in HCT116 cells treated with GH.

We also tested whether GH modifies colon cell survival following etoposide treatment using clonogenic survival assays. Cells were pretreated with GH for 6 hours and treated with etoposide for 1, 3, or 24 hours; fresh GH was added every third day, and colonies were assessed 8 days after the end of etoposide treatment. Fewer colonies were detected in GH-pretreated cells compared with etoposide-only–treated cells (Figure 8A), indicating that, despite acute antiapoptotic effects of GH (54, 55), accumulation of DNA damage in GH-treated cells eventually may result in further cell death.

The ability to survive and grow in the absence of extracellular matrix anchorage correlates closely with tumorigenicity in animal models (56). We examined GH action on soft agar colony formation by pretreating hNCC with 2 different doses of GH (100 and 500 ng/ml) for 6 hours and then treating with etoposide for 1, 3, and 24 hours. Fresh GH was added every third day. In cells treated with etoposide for 3 and 24 hours, both concentrations of GH significantly increased the number of colonies compared with cells treated with etoposide only (Figure 8B), suggesting that GH enhances neoplastic transformation of normal colon cells that survive DNA damage.

GH effects on metastasis in vivo. To confirm these results in vivo, athymic nude mice were injected with HCT116 cells stably infected with lentiGH or lentiV. Four weeks after injection, when xenografted tumors reached ~0.5^3 cm volume, we implanted intrasplenic HCT116 cells to recapitulate the metastatic process, as described (57, 58). Four weeks after intrasplenic injection, mice were sacrificed, and circulating GH was measured to confirm increased levels (Supplemental Figure 10B). Distant pleural, ovarian, and peritoneal metastases were detected in 7 of 9 mice with high-circulating GH, compared with metastases observed in 3 of 10 control animals bearing lentiV xenografts (Figure 8C). There was a strong overall correlation between metastasis count and GH levels (Pearson's correlation = 0.4857, $P = 0.0350$). After adjusting for GH levels, the lentiGH group developed significantly more metastases than the lentiV group (Figure 8D).

Discussion

In this study, we examined effects of GH in nontumorous colon epithelial cells and tissues, using etoposide as a tool to activate DDR. We show that GH acts to attenuate DDR by inhibiting ATM kinase activity; decreasing phosphorylation of key DDR effector proteins including Chk2, p53, and H2AX; and resulting in increased unrepaired DNA. We found that GH reduced NHEJ by more than 30%, thus disrupting normal DNA repair mechanisms.

Loss of genomic integrity due to DDR inactivation may enhance the risk of accumulating oncogenic mutations. Early-stage human colon tumors show elevated levels of DNA damage, which contributes to neoplastic cell growth and proliferation (59, 60). Our results suggest that normal colon cells with GH-induced unrepaired DNA damage are more likely to undergo neoplastic transformation, increasing anchorage-independent growth in vitro and metastasis development in vivo. This hypothesis is reinforced by our findings that the number of metastases correlates strongly with the levels of circulating GH.

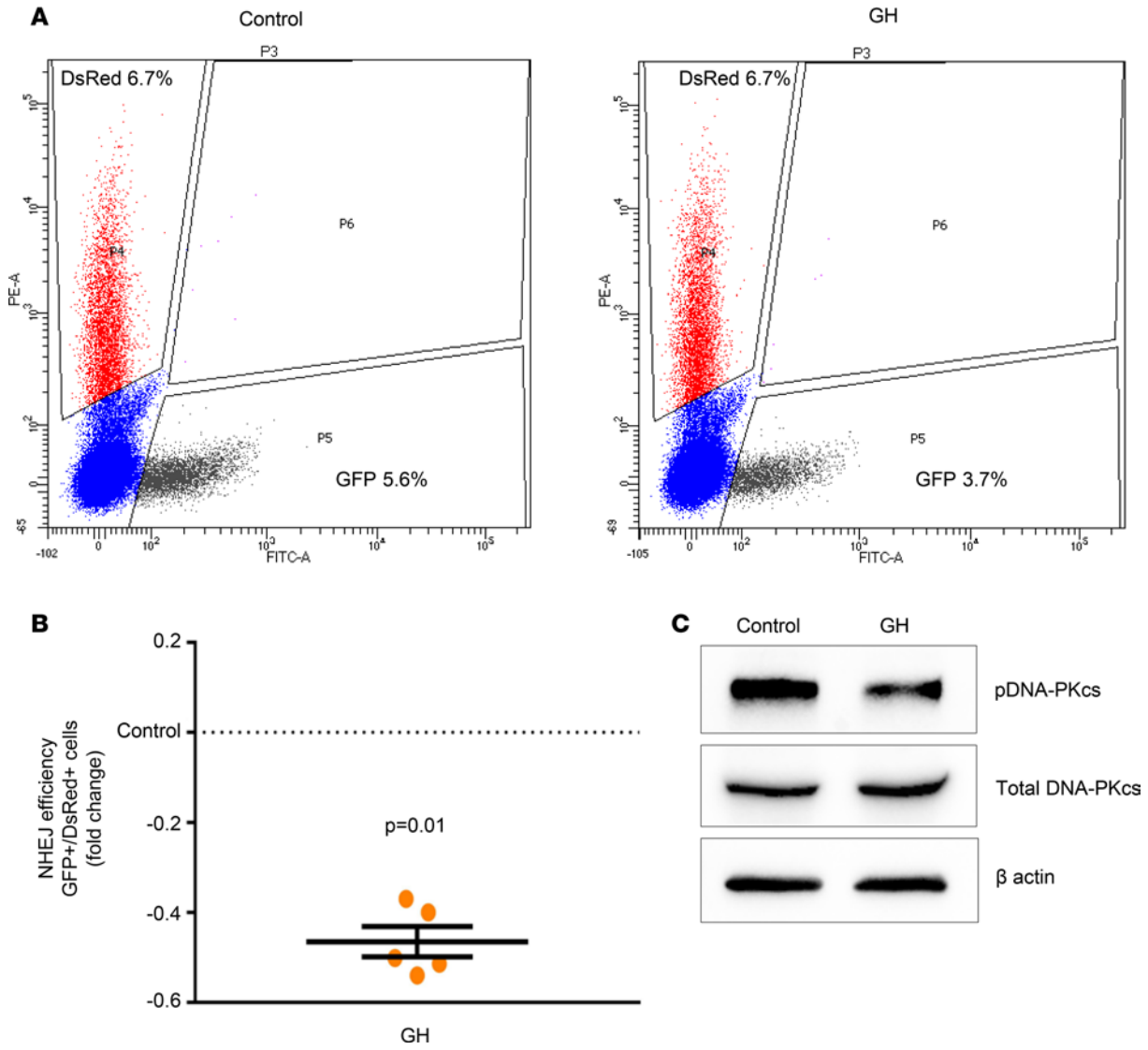

Figure 7. GH attenuates endogenous NHEJ DNA repair by inhibiting DNA-PKcs phosphorylation. (**A**) hNCC containing a chromosomally integrated NHEJ reporter cassette were cotransfected with I-SceI and DsRed expression vectors and treated with 500 ng/ml GH overnight. The intact reporters are negative for GFP. Upon induction of a DSB by I-SceI digestion, the functional GFP gene is reconstituted. Cells were also transfected with pDsRed2-N1 as transfection control, and the percent of DsRed$^+$ cells indicates transfection efficiency. Cells were analyzed by FACS on day 5 after GH treatment, and the relative efficiency of DNA DSB repair was calculated as the ratio of GFP$^+$ cells/DsRed$^+$ cells. Representative analysis is shown. (**B**) Graph shows fold change in GFP positivity ± SEM in 5 independent assays. Controls represent cells not treated with GH. Differences were assessed with Tukey-adjusted mixed model regression. (**C**) Western blot analysis of DNA-PKcs phosphorylation in hNCC treated with 500 ng/ml GH for 24 hours. Representative blots from 5 independent experiments are shown. Quantification of protein expression is depicted in Supplemental Figure 12.

Previous studies have linked the GH/IGF-1 axis with the DNA damage pathway. In prostate cancer cells lines, IGF-1 receptor (IGF-1R) influences DNA repair via DSB repair pathways, while IGF-1R depletion impairs ATM kinase activity in murine melanoma cells and enhances radiosensitivity in human prostate cancer cells (61, 62). GH treatment protects Chinese hamster ovary–4 cells from γ-irradiation (63), and administration of human GH shields normal rat intestinal tissue but not adenocarcinoma xenografts from radiotherapy-induced damage (64, 65). We show here that colon cells treated with GH exhibit suppressed DDR pathways and increased unrepaired DNA damage both at baseline and after stimulation by etoposide. Mice subjected to prolonged high-circulating GH due to GH-secreting xenografts showed ~60% more unrepaired DNA damage in colon tissue, potentially enabling a mucosal microenvironment permissive for transformation. Moreover, we also show that endogenous DNA damage is decreased in colon cells when GHR signaling is blocked. These results were confirmed in vivo in the colon of male *GHR*$^{-/-}$ mice, consistent with previous observations showing that GH-deficient Snell

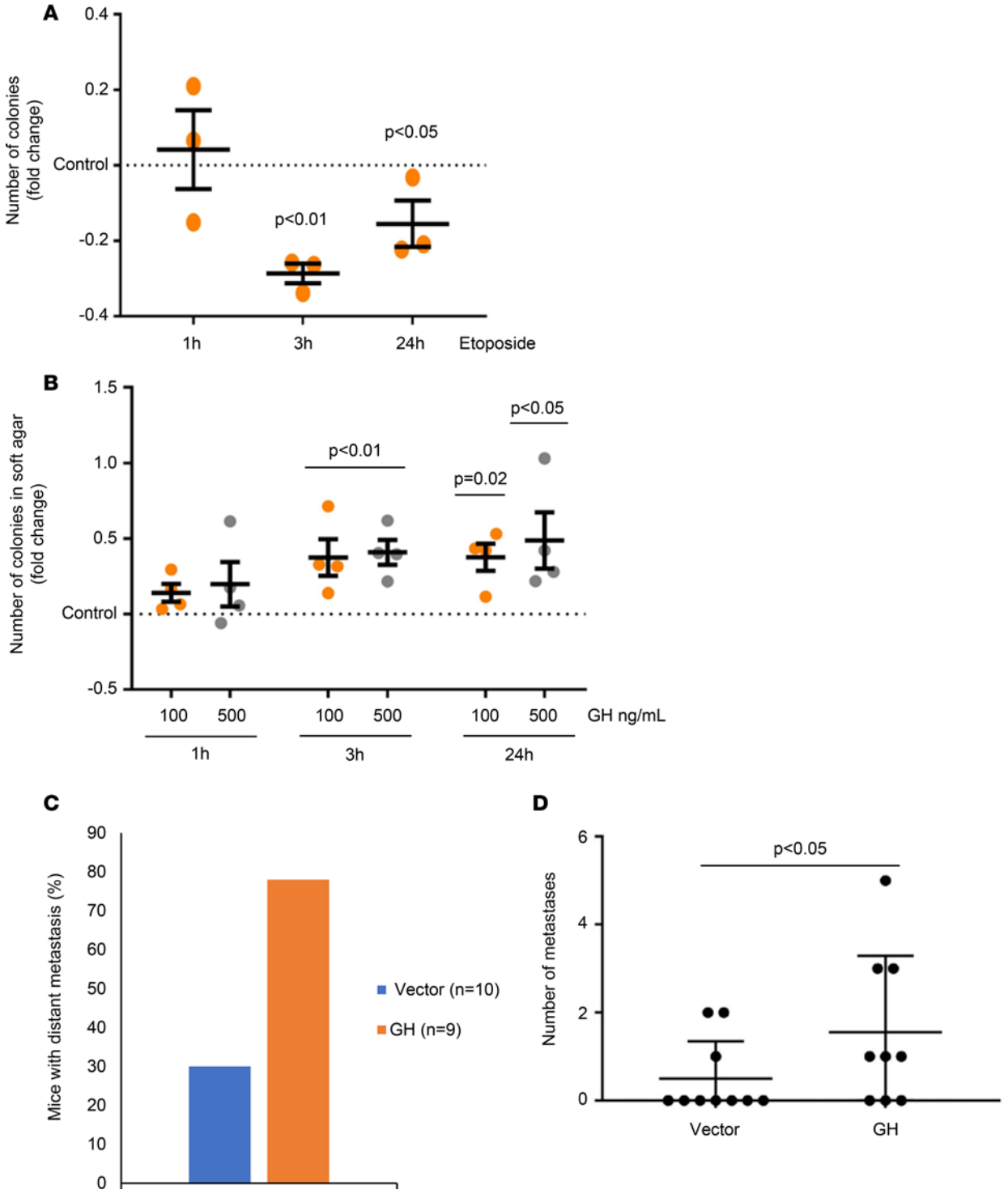

Figure 8. GH decreases survival but increases anchorage-independent growth and metastasis. (**A**) Number of colonies per well in hNCC pretreated with 500 ng/ml for 6 hours and treated with etoposide for 1, 3, and 24 hours and normalized to number of colonies in etoposide-only treated cells (control). The number of colonies was assessed 8 days later, and assays were performed in triplicate. Results shown are mean ± SEM of 3 independent experiments. Controls represent untreated cells. (**B**) Number of colonies formed by hNCC in soft agar treated as in **A** with 100 and 500 ng/ml GH. Results shown are mean ± SEM of duplicates in 4 independent experiments. In **A** and **B**, differences were assessed with Tukey-adjusted mixed model regression. Controls represent cells treated with etoposide only. (**C–D**) Athymic nude mice were injected with HCT116 lenti mGH (GH) or HCT116 lenti vector (vector) cells. Four weeks later, when mice develop ~0.5^3 cm xenograft tumors, they received intrasplenic injections of 500,000 HCT116 cells and were sacrificed 4 weeks later. (**C**) Percent of mice that developed distant metastasis. (**D**) Number of metastases per mouse adjusted to the circulating GH levels. One-way ANCOVA, F = 4.66, degrees of freedom = 1.16, P = 0.045.

dwarf and GHR-KO mice have increased expression of hepatic proteins associated with DNA repair (66). Thus, the effects of GH on DDR are mediated by GHR. Although the exact downstream pathway is yet unknown, it was shown that KRAS is required for GHR-mediated activation of p44/p42 MAPK (67) and that the KRAS/MAPK/ERK pathway is important for radiation resistance (68).

We found that high GH leads to increased unrepaired DNA damage. Some cells that accumulate DNA damage eventually die due to late triggering of apoptosis, as observed in colon cells overexpressing GH (32) and evidenced by reduced colony formation in cells treated with both etoposide and GH compared with etoposide alone. P53 phosphorylation and stabilization results in temporal proliferation block to allow cells to repair DNA damage (69, 70). We previously showed that GH suppresses total p53 (24). Here, we show that GH also reduces ATM activity and destabilizes p53, thus enabling some cells to evade p53-dependent senescence or apoptosis (71, 72) and to continue proliferating despite accumulation of unrepaired DNA damage. Our finding that GH increases the number of hNCC cells entering S phase after etoposide treatment suggests that, by destabilizing p53, GH unblocks replication delay induced by etoposide-activated DNA damage and supports our hypothesis that high GH, by suppressing DDR and DNA repair, allows damaged cells to replicate.

Either upregulated or downregulated/mutated DDR proteins are associated with metastasis (73). Thus, p53 downregulation or mutation induces epithelial mesenchymal transition, migration, and invasion and also inhibits p63, resulting in increased trafficking of β1-integrin, which is intimately involved in metastasis in human breast and prostate carcinomas (74, 75). Downregulation of Tip60 is associated with distant metastases in colon cancer (76) and melanoma (77), and Tip60 overexpression in melanoma cells reduces in vitro cell migration (77). We show here that GH acts to decrease both p53 phosphorylation, as well as Tip60 expression. GH-treated cells demonstrate increased capacity for anchorage-independent growth, consistent with our in vivo results showing increased metastatic potential of colon cells in the presence of high-circulating GH. Others have shown that high GH increased murine pulmonary melanoma metastases (78). These prometastatic effects may be attributed to both GH-mediated DDR suppression and EMT activation (24).

We previously found that in vitro GH treatment and overexpression did not affect IGF-1 or IGF-1R in colon cells (24). However, we cannot exclude that our observed in vivo effects of GH on DDR in colon may also be mediated by IGF-1 signaling, especially as IGF-1R also interacts with the GHR and may augment GH signaling (79). p53 activates IGF-1 binding protein 3 (IGFBP3), which suppresses IGF-1 function (80), and transcriptionally activates IGF-1R (81, 82). GH-induced p53 destabilization may suppress both IGFBP3 and IGF-1R, and decreased IGF-1R may attenuate DNA repair, as has been reported in prostate cancer cell lines (62).

GH action on DDR elucidated here may be cell type specific or specific to normal nontumorous cells with intact DNA damage pathways, as opposed to neoplastic cells harboring multiple mutations. In our studies, GH-induced DNA damage was observed in nontumorous colon and breast cells with intact p53 and DNA damage pathway signaling and in normal human organoids, while less profound effects were found in colon adenocarcinoma HCT116 cells that exhibit DNA repair alterations (83). Others have demonstrated ATM and H2AX phosphorylation in GH-treated malignant basal prostate cells, but only moderate effects on luminal cells (84), as well as decreased DNA damage and increased cell survival with GH overexpression in human endometrial and mammary carcinoma cells (85). Thus, GH effects may differ in normal and malignant tumor cells. In addition, protective effects of GH in DNA damaged cells may be also associated with clearing of chemotherapeutic drug. Although we show that GH does not affect MDR1 expression in hNCC, GH treatment of human melanoma cells induced expression of ATP-binding xenobiotic efflux pumps associated with melanoma drug resistance (86).

We elucidated mechanisms underlying GH effects on ATM. ATM can be regulated via different pathways. After DNA damage, the Mre11/Rad50/Nbs1 (MRN) DNA-binding complex is required for ATM activation (87), and spectrometry-based phosphoproteomics showed that GH rapidly dephosphorylates Mre11 and Rad50 in 3T3-F442A preadipocytes, potentially affecting activity of the MRN complex (88). TRIM29, induced by DNA damage, binds and degrades the histone acetyltransferase Tip60 (46), which also induces ATM kinase activity in response to DNA damage. Suppression of Tip60 blocks ATM kinase activity and prevents ATM-dependent phosphorylation of p53 and Chk2 (42), and Tip60 downregulation is linked to development of advanced colorectal carcinomas (76). We show here that GH markedly induces normal colon cell TRIM29, leading to decreased Tip60 expression, diminished ATM phosphorylation, and prevention of DDR from being fully activated in response to DNA damaging treatment. By contrast, suppression of baseline TRIM29 in hNCC resulted in Tip60 induction with subsequent ATM activation. Further confirming the importance of GH signaling for this pathway, pharmacological blockade of the GHR abolished TRIM29 and induced Tip60 expression, with

induced phosphorylation of ATM and p53. Cellular responses to DNA damaging agents is complex. TRIM29 has several functions in tumorigenesis, depending on cell and tissue type (89), including acting as a scaffold protein for DNA repair proteins (41). The mutual relationship between TRIM29 and Tip60 is not clear-cut in cells exposed to etoposide. However, the results shown here suggest that GH induces TRIM29 and suppresses Tip60, and may be at least partially responsible for decreased ATM phosphorylation in cells treated with both etoposide and GH. Mechanisms underlying GH effects on TRIM29 expression are yet unknown.

ATM orchestrates cellular responses to DNA damage by activating checkpoint molecules, apoptosis, senescence, chromatin structure alterations, and DNA repair, while the primary role of DNA-PK is to promote NHEJ (33, 90). MRN-dependent ATM stimulation triggers phosphorylation of DNA-PKcs to induce NHEJ, while also directly promoting HR (91). Although we cannot exclude other pathways for reduction of DNA-PKcs phosphorylation, we detected reduced DNA-PKcs phosphorylation with decreased NHEJ in cells treated with GH, suggesting that GH action on DNA-PKcs may be mediated by decreased ATM activity.

Acromegaly patients with high ambient circulating GH levels develop colon polyps and other soft tissue tumors (21, 22) and have increased risk for developing colon adenocarcinoma (22). As colon polyp and adenoma frequency also significantly increase with age (92), our results point to the risk of GH replacement therapy in pituitary-replete healthy adults. As functional DDR pathways and adequate DNA repair are protective against neoplastic insults (93), GH administration to pituitary-replete adults may confer an unacceptable risk for epithelial proliferation and could contribute to field cancerization due to colon epithelial cell reprograming (94). In line with this hypothesis, short-stature adults with Laron syndrome (28), as well as animals with GHR deficiency (20, 29, 95), are protected from developing neoplasms.

Our results identify potentially novel mechanisms underlying protumorigenic properties of high GH levels. These results raise awareness that long-term inappropriate GH treatment may present a risk of developing colon epithelial cell transformation, as well as activation of preexisting low-grade tumors.

Methods

Supplemental methods are available online with this article.

Mice

Animal experiments were approved by the Cedars-Sinai Institutional Animal Care and Use Committee (IACUC 5587). *GHR*$^{-/-}$ mice (B6N[Cg]-*Ghr*$^{tm1b[KOMP]wtsi/3J}$) were purchased from The Jackson Laboratory. Breeding was performed with heterozygous males and females so WT and *GHR*$^{-/-}$ mice were obtained from the same breeding. In the course of breeding, heterozygous mice were backcrossed with WT mice at least 5 times.

Xenograft model. HCT116 cells stably infected with lenti-murine GH (5×10^5 cells in 0.05 ml PBS) were mixed (1:1) with Matrigel (Corning) and injected s.c. into the right flank of athymic nude female mice (The Jackson Laboratory) to establish a model of excess systemic GH. Control mice were injected with HCT116 cells infected with empty vector. All mice developed xenograft tumors. Increased circulating GH and IFG-1 levels were confirmed with ELISA (MilliporeSigma).

Experimental metastases. A colorectal cancer mouse model exhibiting spontaneous metastases originating from intrasplenic primary tumor was employed (57, 96). When xenograft tumors reached 0.5^3 cm, HCT116 cells (500,000 cells/100 μl PBS per animal) were injected into the spleen of xenograft bearing mice. Each group included 14 animals. Mice were weighed once a week, and metastasis development was monitored. Four weeks later, mice were sacrificed and abdominal organs examined for metastases. One mouse from the lentiGH group developed abdominal abscess, had to be euthanized 1 weeks after intraspleen injection, and was excluded from the study.

Cells and treatments

Human colon carcinoma HCT116 cells and human nontumorous breast cells (MCF12A) were obtained from American Type Culture Collection (ATCC). HCT116 were cultured in McCoy's 5A medium (Invitrogen) and 10% FBS. MCF12A were cultured in DMEM/F12 medium (Invitrogen) with 0.5 μg/ml hydrocortisone (MilliporeSigma), 10 μg/ml insulin (MilliporeSigma), 20 ng/ml EGF (Invitrogen), and 5% horse serum (Omega Scientific). hNCC were purchased (Applied Biological Materials) and cultured in PriGrow III Media (Applied Biological Materials) supplemented with 5% FBS. All media were supplemented with antibiotic/antimycotic solution from Gemini Bio-Products. Cells were infected or treated before passage 4, per manufacturer instruction.

Pegvisomant was donated by Pfizer (to SM). Etoposide (MilliporeSigma) was prepared as a 10 mM DMSO stock solution. Cells and 3-dimensional intestinal organoids were treated at the indicated doses for the indicated times. Recombinant human GH1 (Biovision) was reconstituted in PBS pH8 containing 0.1% BSA. Cells were placed in culture medium free of serum containing 0.1% BSA, GH was added at a concentration of 500 ng/ml, and cells were harvested at the indicated times.

Three-dimensional intestinal organoids

Fibroblasts were obtained from healthy human volunteer donors at Cedars-Sinai (IRB, 00027264). Three-dimensional intestinal organoids were generated from a control fibroblast 83i induced pluripotent stem cell (iPSC) line using an episomal plasmid reprogramming system. To induce definitive endoderm formation, all iPSCs were cultured with a high dose of activin A (100 ng/ml; R&D Systems) with increasing concentrations of FBS over time (0%, 0.2%, and 2% [vol/vol] on days 1, 2, and 3, respectively). Wnt3A (25 ng/ml; R&D Systems) was also added on the first day of endoderm differentiation. To induce hindgut formation, cells were cultured in advanced DMEM/F12 with 2% (vol/vol) FBS, along with CHIR 99021 (2 μM; Tocris) and FGF4 (500 ng/ml; R&D Systems). After 3–4 days, free-floating epithelial spheres and loosely attached epithelial tubes became visible and were harvested. Epithelial structures were subsequently suspended in Matrigel and then overlaid in intestinal medium containing CHIR99021 (2 μM; Tocris), noggin, EGF (both 100 ng/ml; both R&D Systems), and B27 (1×; Invitrogen). Organoids were passaged every 7–10 days thereafter (97).

Image analysis of γH2AX with CellProfiler

To analyze γH2AX intensity, we pretreated hNCC with 500 ng/ml GH for 6 hours and then treated with 5 μM etoposide. Twenty-four hours after etoposide treatment, cells were fixed and confocal images analyzed using the MIT CellProfiler software (Carpenter Genome Biology 2006 7:R100) using the Speckle Counting analysis pipeline (http://cellprofiler.org/examples/#Speckles), which identifies intranuclear foci and computes per-object aggregate measurements, including number of foci per nucleus and intensities. Confocal images were analyzed without speckle-enhancer processing. Cells with intense nonfocal γH2AX signals that may reflect apoptosis were excluded from analysis. Twenty to 30 nuclei per image, and 5 images per group, were analyzed. Speckle intensity measurements were then further analyzed (98).

DSB repair assays

DSB repair was assessed as described (52, 99). Briefly, NHEJ reporter cassette and HR reporter cassette were chromosomally integrated in hNCC. hNCC were nucleofected with DNA reporter cassettes using Amaxa Basic Nucleofector Kit for Primary Mammalian Epithelial Cells (Lonza, catalog VPI-1005) in Amaxa Nucleofector-I (Lonza, program no. W-01). These cassettes contain the GFP gene with recognition sequences for I-SceI endonucleases for induction of DSBs. Stably transfected cells were selected for 10 days with 1 mg/ml of G418 and then cotransfected (by nucleofection) with 5 μg plasmid encoding I-SceI endonuclease (pCBASceI; Addgene, plasmid no. 26477) to induce DSBs, and 0.5 μg plasmid encoding DsRed (pDsRed2-N1; Clontech) to control for transfection efficiency. Intact reporters are negative for GFP. Upon induction of a DSB by I-SceI digestion, the functional GFP gene was reconstituted. The percent of GFP^+ cells corresponds to the efficiency of DNA DSB repair, and the percent of $DsRed^+$ cells indicates the efficiency of transfection. Five days after transfection, the number of GFP^+ and $DsRed^+$ cells was determined by flow cytometry. The ratio between GFP^+ and $DsRed^+$ cells was used as a measure of DSB repair efficiency. In hNCC, NHEJ repair efficiency was 0.77–0.83, and HR efficiency was approximately 0.05 in control cells, which is consistent with other reports (39, 43, 44). FACS analysis was performed using FACSCanto (BD Biosciences). For each treatment, a minimum of 50,000 cells was analyzed by FACS. Final data analysis was done using FlowJo software.

Statistics

Aggregate measurements of γH2AX foci were analyzed by nonparametric Wilcoxon rank sum test. In all other experiments, differences between groups were tested with mixed model regression to allow for random effects of intra-assay variation. Post hoc testing was performed with Tukey's test to control for multiple comparisons. Residuals were inspected to confirm that data met assumptions necessary for parametric testing. Image quantification in colon tissue was assessed using 2-tailed Student's *t* test. Differences were

considered significant where $P < 0.05$. Data are graphed as fold-change or percent of control, but statistical testing was performed on raw numbers. For metastases, analysis data were log-transformed prior to analysis to meet assumptions necessary for parametric testing. Differences in number of tumors was tested between groups in one-way ANCOVA to adjust for circulating levels of GH.

Study approval

Animal experiments were approved by the Cedars-Sinai Institutional Animal Care and Use Committee (IACUC, 5587). Generation of iPSC from fibroblasts obtained from healthy human volunteer donors at Cedars-Sinai was approved by the Cedars-Sinai Medical Center IRB (no. 00027264).

Author contributions

VC, SZ, HK, RB, JG, and MY conducted experiments; KW acquired and analyzed data; VC, ABS, and SM analyzed, discussed, and interpreted the data; CB performed statistical analysis; and VG provided reagents and analyzed, discussed, and interpreted the data. VC and SM developed the hypothesis and wrote the manuscript. SM coordinated and directed the project. All authors approved the submitted manuscript.

Acknowledgments

This work was supported by NIH grants DK103198, DK007770, and AG047200; Pfizer ASPIRE Award WI215910; and the Doris Factor Molecular Endocrinology Laboratory at Cedars-Sinai. We are grateful to Shira Berman for assistance with manuscript preparation.

Address correspondence to: Shlomo Melmed, Academic Affairs, Room 2015, Cedars-Sinai Medical Center, 8700 Beverly Boulevard, Los Angeles, California 90048, USA. Phone: 310.423.4691; Email: melmed@csmc.edu.

1. Ceseña TI, et al. Multiple mechanisms of growth hormone-regulated gene transcription. *Mol Genet Metab*. 2007;90(2):126–133.
2. Lanning NJ, Carter-Su C. Recent advances in growth hormone signaling. *Rev Endocr Metab Disord*. 2006;7(4):225–235.
3. Chia DJ. Minireview: mechanisms of growth hormone-mediated gene regulation. *Mol Endocrinol*. 2014;28(7):1012–1025.
4. Clayton PE, Gill MS, Tillmann V, Westwood M. Translational neuroendocrinology: control of human growth. *J Neuroendocrinol*. 2014;26(6):349–355.
5. Yakar S, Isaksson O. Regulation of skeletal growth and mineral acquisition by the GH/IGF-1 axis: Lessons from mouse models. *Growth Horm IGF Res*. 2016;28:26–42.
6. Giustina A, Mazziotti G, Canalis E. Growth hormone, insulin-like growth factors, and the skeleton. *Endocr Rev*. 2008;29(5):535–559.
7. Chikani V, Ho KK. Action of GH on skeletal muscle function: molecular and metabolic mechanisms. *J Mol Endocrinol*. 2014;52(1):R107–R123.
8. Miquet JG, et al. Hepatocellular alterations and dysregulation of oncogenic pathways in the liver of transgenic mice overexpressing growth hormone. *Cell Cycle*. 2013;12(7):1042–1057.
9. Molitch ME, Clemmons DR, Malozowski S, Merriam GR, Vance ML, Endocrine Society. Evaluation and treatment of adult growth hormone deficiency: an Endocrine Society clinical practice guideline. *J Clin Endocrinol Metab*. 2011;96(6):1587–1609.
10. Yamamoto H, Sohmiya M, Oka N, Kato Y. Effects of aging and sex on plasma insulin-like growth factor I (IGF-I) levels in normal adults. *Acta Endocrinol*. 1991;124(5):497–500.
11. Milman S, Huffman DM, Barzilai N. The Somatotropic Axis in Human Aging: Framework for the Current State of Knowledge and Future Research. *Cell Metab*. 2016;23(6):980–989.
12. Bartke A. Growth hormone and aging: a challenging controversy. *Clin Interv Aging*. 2008;3(4):659–665.
13. Bartke A. Declining sperm counts and increases in testicular cancer: a legacy of the cold war? *J Androl*. 2009;30(3):213.
14. Salomon F, Cuneo RC, Hesp R, Sönksen PH. The effects of treatment with recombinant human growth hormone on body composition and metabolism in adults with growth hormone deficiency. *N Engl J Med*. 1989;321(26):1797–1803.
15. Giordano R, Bonelli L, Marinazzo E, Ghigo E, Arvat E. Growth hormone treatment in human ageing: benefits and risks. *Hormones (Athens)*. 2008;7(2):133–139.
16. Liu H, et al. Systematic review: the effects of growth hormone on athletic performance. *Ann Intern Med*. 2008;148(10):747–758.
17. Blackman MR, et al. Growth hormone and sex steroid administration in healthy aged women and men: a randomized controlled trial. *JAMA*. 2002;288(18):2282–2292.
18. Anisimov VN, Bartke A. The key role of growth hormone-insulin-IGF-1 signaling in aging and cancer. *Crit Rev Oncol Hematol*. 2013;87(3):201–223.
19. Waters MJ, Brooks AJ. Growth hormone and cell growth. *Endocr Dev*. 2012;23:86–95.
20. Junnila RK, List EO, Berryman DE, Murrey JW, Kopchick JJ. The GH/IGF-1 axis in ageing and longevity. *Nat Rev Endocrinol*. 2013;9(6):366–376.
21. Melmed S. Acromegaly pathogenesis and treatment. *J Clin Invest*. 2009;119(11):3189–3202.
22. Lois K, Bukowczan J, Perros P, Jones S, Gunn M, James RA. The role of colonoscopic screening in acromegaly revisited:

review of current literature and practice guidelines. *Pituitary*. 2015;18(4):568–574.
23. Dal J, et al. Cancer Incidence in Patients With Acromegaly: A Cohort Study and Meta-Analysis of the Literature. *J Clin Endocrinol Metab*. 2018;103(6):2182–2188.
24. Chesnokova V, et al. Growth hormone is permissive for neoplastic colon growth. *Proc Natl Acad Sci USA*. 2016;113(23):E3250–E3259.
25. Brittain AL, Basu R, Qian Y, Kopchick JJ. Growth Hormone and the Epithelial-to-Mesenchymal Transition. *J Clin Endocrinol Metab*. 2017;102(10):3662–3673.
26. Wang JJ, et al. Autocrine hGH stimulates oncogenicity, epithelial-mesenchymal transition and cancer stem cell-like behavior in human colorectal carcinoma. *Oncotarget*. 2017;8(61):103900–103918.
27. Perry JK, Liu DX, Wu ZS, Zhu T, Lobie PE. Growth hormone and cancer: an update on progress. *Curr Opin Endocrinol Diabetes Obes*. 2013;20(4):307–313.
28. Guevara-Aguirre J, et al. Growth hormone receptor deficiency is associated with a major reduction in pro-aging signaling, cancer, and diabetes in humans. *Sci Transl Med*. 2011;3(70):70ra13.
29. Ikeno Y, Bronson RT, Hubbard GB, Lee S, Bartke A. Delayed occurrence of fatal neoplastic diseases in ames dwarf mice: correlation to extended longevity. *J Gerontol A Biol Sci Med Sci*. 2003;58(4):291–296.
30. Carroll RE, et al. Reduced susceptibility to azoxymethane-induced aberrant crypt foci formation and colon cancer in growth hormone deficient rats. *Growth Horm IGF Res*. 2009;19(5):447–456.
31. Basu R, Wu S, Kopchick JJ. Targeting growth hormone receptor in human melanoma cells attenuates tumor progression and epithelial mesenchymal transition via suppression of multiple oncogenic pathways. *Oncotarget*. 2017;8(13):21579–21598.
32. Chesnokova V, et al. Growth hormone is a cellular senescence target in pituitary and nonpituitary cells. *Proc Natl Acad Sci USA*. 2013;110(35):E3331–E3339.
33. Blackford AN, Jackson SP. ATM, ATR, and DNA-PK: The Trinity at the Heart of the DNA Damage Response. *Mol Cell*. 2017;66(6):801–817.
34. Bakkenist CJ, Kastan MB. DNA damage activates ATM through intermolecular autophosphorylation and dimer dissociation. *Nature*. 2003;421(6922):499–506.
35. Smith J, Tho LM, Xu N, Gillespie DA. The ATM-Chk2 and ATR-Chk1 pathways in DNA damage signaling and cancer. *Adv Cancer Res*. 2010;108:73–112.
36. Rashi-Elkeles S, et al. Transcriptional modulation induced by ionizing radiation: p53 remains a central player. *Mol Oncol*. 2011;5(4):336–348.
37. Ciccia A, Elledge SJ. The DNA damage response: making it safe to play with knives. *Mol Cell*. 2010;40(2):179–204.
38. Shiloh Y, Ziv Y. The ATM protein kinase: regulating the cellular response to genotoxic stress, and more. *Nat Rev Mol Cell Biol*. 2013;14(4):197–210.
39. Rogakou EP, Pilch DR, Orr AH, Ivanova VS, Bonner WM. DNA double-stranded breaks induce histone H2AX phosphorylation on serine 139. *J Biol Chem*. 1998;273(10):5858–5868.
40. Turinetto V, Giachino C. Multiple facets of histone variant H2AX: a DNA double-strand-break marker with several biological functions. *Nucleic Acids Res*. 2015;43(5):2489–2498.
41. Masuda Y, et al. TRIM29 regulates the assembly of DNA repair proteins into damaged chromatin. *Nat Commun*. 2015;6:7299.
42. Sun Y, Jiang X, Chen S, Fernandes N, Price BD. A role for the Tip60 histone acetyltransferase in the acetylation and activation of ATM. *Proc Natl Acad Sci USA*. 2005;102(37):13182–13187.
43. Walles SA, Zhou R, Liliemark E. DNA damage induced by etoposide; a comparison of two different methods for determination of strand breaks in DNA. *Cancer Lett*. 1996;105(2):153–159.
44. Gatei M, et al. ATM protein-dependent phosphorylation of Rad50 protein regulates DNA repair and cell cycle control. *J Biol Chem*. 2011;286(36):31542–31556.
45. Turinetto V, Giachino C. Histone variants as emerging regulators of embryonic stem cell identity. *Epigenetics*. 2015;10(7):563–573.
46. Sho T, et al. TRIM29 negatively regulates p53 via inhibition of Tip60. *Biochim Biophys Acta*. 2011;1813(6):1245–1253.
47. Thiebaut F, Tsuruo T, Hamada H, Gottesman MM, Pastan I, Willingham MC. Cellular localization of the multidrug-resistance gene product P-glycoprotein in normal human tissues. *Proc Natl Acad Sci USA*. 1987;84(21):7735–7738.
48. Kopchick JJ, Parkinson C, Stevens EC, Trainer PJ. Growth hormone receptor antagonists: discovery, development, and use in patients with acromegaly. *Endocr Rev*. 2002;23(5):623–646.
49. Jackson SP, Bartek J. The DNA-damage response in human biology and disease. *Nature*. 2009;461(7267):1071–1078.
50. Beucher A, et al. ATM and Artemis promote homologous recombination of radiation-induced DNA double-strand breaks in G2. *EMBO J*. 2009;28(21):3413–3427.
51. Chapman JR, Taylor MR, Boulton SJ. Playing the end game: DNA double-strand break repair pathway choice. *Mol Cell*. 2012;47(4):497–510.
52. Seluanov A, Mao Z, Gorbunova V. Analysis of DNA double-strand break (DSB) repair in mammalian cells. *J Vis Exp*. 2010;(43):2002.
53. Smith GC, Jackson SP. The DNA-dependent protein kinase. *Genes Dev*. 1999;13(8):916–934.
54. Jeay S, Sonenshein GE, Postel-Vinay MC, Baixeras E. Growth hormone prevents apoptosis through activation of nuclear factor-kappaB in interleukin-3-dependent Ba/F3 cell line. *Mol Endocrinol*. 2000;14(5):650–661.
55. Bogazzi F, et al. Growth hormone inhibits apoptosis in human colonic cancer cell lines: antagonistic effects of peroxisome proliferator activated receptor-gamma ligands. *Endocrinology*. 2004;145(7):3353–3362.
56. Carney DN, Gazdar AF, Minna JD. Positive correlation between histological tumor involvement and generation of tumor cell colonies in agarose in specimens taken directly from patients with small-cell carcinoma of the lung. *Cancer Res*. 1980;40(6):1820–1823.
57. Lavilla-Alonso S, et al. Optimized mouse model for the imaging of tumor metastasis upon experimental therapy. *PLoS One*. 2011;6(11):e26810.
58. Zhou C, Tong Y, Wawrowsky K, Melmed S. PTTG acts as a STAT3 target gene for colorectal cancer cell growth and motility. *Oncogene*. 2014;33(7):851–861.
59. Bartek J, Bartkova J, Lukas J. DNA damage signalling guards against activated oncogenes and tumour progression. *Oncogene*.

2007;26(56):7773–7779.
60. Meira LB, et al. DNA damage induced by chronic inflammation contributes to colon carcinogenesis in mice. *J Clin Invest*. 2008;118(7):2516–2525.
61. Chitnis MM, Lodhia KA, Aleksic T, Gao S, Protheroe AS, Macaulay VM. IGF-1R inhibition enhances radiosensitivity and delays double-strand break repair by both non-homologous end-joining and homologous recombination. *Oncogene*. 2014;33(45):5262–5273.
62. Turney BW, et al. Depletion of the type 1 IGF receptor delays repair of radiation-induced DNA double strand breaks. *Radiother Oncol*. 2012;103(3):402–409.
63. Madrid O, et al. Growth hormone protects against radiotherapy-induced cell death. *Eur J Endocrinol*. 2002;147(4):535–541.
64. Caz V, et al. Growth Hormone Protects the Intestine Preserving Radiotherapy Efficacy on Tumors: A Short-Term Study. *PLoS One*. 2015;10(12):e0144537.
65. Morante J, et al. Differential action of growth hormone in irradiated tumoral and nontumoral intestinal tissue. *Dig Dis Sci*. 2003;48(11):2159–2166.
66. Dominick G, Bowman J, Li X, Miller RA, Garcia GG. mTOR regulates the expression of DNA damage response enzymes in long-lived Snell dwarf, GHRKO, and PAPPA-KO mice. *Aging Cell*. 2017;16(1):52–60.
67. Zhu T, Goh EL, Graichen R, Ling L, Lobie PE. Signal transduction via the growth hormone receptor. *Cell Signal*. 2001;13(9):599–616.
68. Munshi A, Ramesh R. Mitogen-activated protein kinases and their role in radiation response. *Genes Cancer*. 2013;4(9-10):401–408.
69. Roy S, et al. p53 orchestrates DNA replication restart homeostasis by suppressing mutagenic RAD52 and POLθ pathways. *Elife*. 2018;7:e31723.
70. Fletcher SC, et al. Sp1 phosphorylation by ATM downregulates BER and promotes cell elimination in response to persistent DNA damage. *Nucleic Acids Res*. 2018;46(4):1834–1846.
71. Sarkisian CJ, Keister BA, Stairs DB, Boxer RB, Moody SE, Chodosh LA. Dose-dependent oncogene-induced senescence in vivo and its evasion during mammary tumorigenesis. *Nat Cell Biol*. 2007;9(5):493–505.
72. Mondal AM, et al. p53 isoforms regulate aging- and tumor-associated replicative senescence in T lymphocytes. *J Clin Invest*. 2013;123(12):5247–5257.
73. Corcoran NM, Clarkson MJ, Stuchbery R, Hovens CM. Molecular Pathways: Targeting DNA Repair Pathway Defects Enriched in Metastasis. *Clin Cancer Res*. 2016;22(13):3132–3137.
74. Muller PA, Vousden KH, Norman JC. p53 and its mutants in tumor cell migration and invasion. *J Cell Biol*. 2011;192(2):209–218.
75. Broustas CG, Lieberman HB. DNA damage response genes and the development of cancer metastasis. *Radiat Res*. 2014;181(2):111–130.
76. Sakuraba K, et al. Down-regulation of Tip60 gene as a potential marker for the malignancy of colorectal cancer. *Anticancer Res*. 2009;29(10):3953–3955.
77. Chen G, Cheng Y, Tang Y, Martinka M, Li G. Role of Tip60 in human melanoma cell migration, metastasis, and patient survival. *J Invest Dermatol*. 2012;132(11):2632–2641.
78. Chien CH, Lee MJ, Liou HC, Liou HH, Fu WM. Growth hormone is increased in the lungs and enhances experimental lung metastasis of melanoma in DJ-1 KO mice. *BMC Cancer*. 2016;16(1):871.
79. Gan Y, et al. Human GH receptor-IGF-1 receptor interaction: implications for GH signaling. *Mol Endocrinol*. 2014;28(11):1841–1854.
80. Buckbinder L, et al. Induction of the growth inhibitor IGF-binding protein 3 by p53. *Nature*. 1995;377(6550):646–649.
81. Hinkal G, Donehower LA. How does suppression of IGF-1 signaling by DNA damage affect aging and longevity? *Mech Ageing Dev*. 2008;129(5):243–253.
82. Werner H, Maor S. The insulin-like growth factor-I receptor gene: a downstream target for oncogene and tumor suppressor action. *Trends Endocrinol Metab*. 2006;17(6):236–242.
83. Samuels Y, et al. Mutant PIK3CA promotes cell growth and invasion of human cancer cells. *Cancer Cell*. 2005;7(6):561–573.
84. Zhang Z, et al. Differential epithelium DNA damage response to ATM and DNA-PK pathway inhibition in human prostate tissue culture. *Cell Cycle*. 2011;10(20):3545–3553.
85. Bougen NM, et al. Autocrine human GH promotes radioresistance in mammary and endometrial carcinoma cells. *Endocr Relat Cancer*. 2012;19(5):625–644.
86. Basu R, Baumgaertel N, Wu S, Kopchick JJ. Growth Hormone Receptor Knockdown Sensitizes Human Melanoma Cells to Chemotherapy by Attenuating Expression of ABC Drug Efflux Pumps. *Horm Cancer*. 2017;8(3):143–156.
87. Lee JH, Paull TT. Activation and regulation of ATM kinase activity in response to DNA double-strand breaks. *Oncogene*. 2007;26(56):7741–7748.
88. Ray BN, Kweon HK, Argetsinger LS, Fingar DC, Andrews PC, Carter-Su C. Research resource: identification of novel growth hormone-regulated phosphorylation sites by quantitative phosphoproteomics. *Mol Endocrinol*. 2012;26(6):1056–1073.
89. Hatakeyama S. TRIM proteins and cancer. *Nat Rev Cancer*. 2011;11(11):792–804.
90. Jette N, Lees-Miller SP. The DNA-dependent protein kinase: A multifunctional protein kinase with roles in DNA double strand break repair and mitosis. *Prog Biophys Mol Biol*. 2015;117(2-3):194–205.
91. Jazayeri A, et al. ATM- and cell cycle-dependent regulation of ATR in response to DNA double-strand breaks. *Nat Cell Biol*. 2006;8(1):37–45.
92. Corley DA, et al. Variation of adenoma prevalence by age, sex, race, and colon location in a large population: implications for screening and quality programs. *Clin Gastroenterol Hepatol*. 2013;11(2):172–180.
93. Hanahan D, Weinberg RA. The hallmarks of cancer. *Cell*. 2000;100(1):57–70.
94. Curtius K, Wright NA, Graham TA. An evolutionary perspective on field cancerization. *Nat Rev Cancer*. 2018;18(1):19–32.
95. Bartke A. Growth Hormone and Aging: Updated Review. *World J Mens Health*. 2019;37(1):19–30.
96. Zhou C, Jiao Y, Wang R, Ren SG, Wawrowsky K, Melmed S. STAT3 upregulation in pituitary somatotroph adenomas induces growth hormone hypersecretion. *J Clin Invest*. 2015;125(4):1692–1702.
97. Barrett R, et al. Reliable generation of induced pluripotent stem cells from human lymphoblastoid cell lines. *Stem Cells Transl*

Med. 2014;3(12):1429–1434.
98. Carpenter AE, et al. CellProfiler: image analysis software for identifying and quantifying cell phenotypes. *Genome Biol*. 2006;7(10):R100.
99. Van Meter M, et al. JNK Phosphorylates SIRT6 to Stimulate DNA Double-Strand Break Repair in Response to Oxidative Stress by Recruiting PARP1 to DNA Breaks. *Cell Rep*. 2016;16(10):2641–2650.